AlGaAs nanowires for phase-matched SHG in the telecom range

Natalia MORAIS[1*], Fares CHOUCHANE[1], Marco RAVARO[1], Maurizio DE ROSA[2], Iolanda RICCIARDI[2], Aristide LEMAITRE[3], Ivan FAVERO[1], and Giuseppe LEO[1]

[1] Laboratoire Matériaux et Phénomènes Quantiques, UMR 7162,
Université Paris Diderot – CNRS, Paris, France
[2] INO – CNR, Istituto Nazionale di Ottica, Via Campi Flegrei 34, I-80078 Pozzuoli (NA), Italy
[3] Alcatel-Thales III-V Lab, Palaiseau, France
*natalia.morais@univ-paris-diderot.fr

Phase-matched three-wave mixing is possible in optically isotropic zinc-blende materials, thanks to quasi-phase matching occurring when the interacting fields propagate along a curved path about a principal dielectric axis [1]. Following this scheme, efficient Second Harmonic Generation (SHG) was recently demonstrated in GaAs [2] and AlGaAs microdisks [3], and it was predicted in curved waveguides [4].

We designed and fabricated snake-shaped nanowires for SHG in the optical telecom range, both in fully suspended $Al_{0.19}Ga_{0.81}As$ waveguides and in $Al_{0.19}Ga_{0.81}As$ on aluminium oxide. These waveguides are composed by a series of quarters of a ring, as sketched in Fig. 1. The sign of $\chi^{(2)}$ is inverted every two adjacent 90° arcs. By doing so, it is possible to perform an "effective" quasi-phase matching, without any technological burden associated to $\chi^{(2)}$ domain inversion [1].

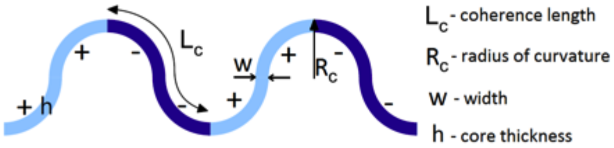

Fig. 1. Parameters for the design of snake-shaped waveguides

The coherence length, L_c, the maximum distance over which the nonlinear interaction is constructive, for SHG, depends on the difference between the effective indices at the second harmonic (SH) and the fundamental frequency (FF):

$$L_c = \frac{\lambda}{4}\frac{1}{n_{\mathrm{SH}}(\lambda_{\mathrm{SH}}, w, h) - n_{\mathrm{FF}}(\lambda_{\mathrm{FF}}, w, h)}, \tag{1}$$

Since these effective indices depend on the geometry of the waveguide (w, h) and $R_c = L_c/\pi$, Eq. 1 relates all the parameters in the waveguide geometry. To minimize propagation losses, one needs $R_c \gg w$, and thus maximise L_c. The coherence length as a function of the wavelength and the width of the waveguide is shown in Fig. 2a for a suspended waveguide and in Fig. 2b for a waveguide on aluminium oxide.

Both samples have been fabricated on a (100) GaAs wafer. For the first one, a 123nm $Al_{0.19}Ga_{0.81}As$ layer is grown over an $Al_{0.80}Ga_{0.20}As$ sacrificial layer, while for the second one, we grow a 100nm $Al_{0.19}Ga_{0.81}As$ layer on an $Al_{0.98}Ga_{0.02}As$ layer to be oxidised after lithography and etching. A few electron-microscope images are shown in Fig. 3.

Both waveguides are excited by a continuous-wave laser at a FF wavelength of 1.55µm, and we collect both FF throughput and SH output at 775nm with lock-in detection. End-fire input and output light coupling is performed via micro-lensed fibres and inverted tapers. The latter, of the type shown in Fig. 3b, are optimized for FF TE-polarized light at the input and SH TM-polarized light at the output.

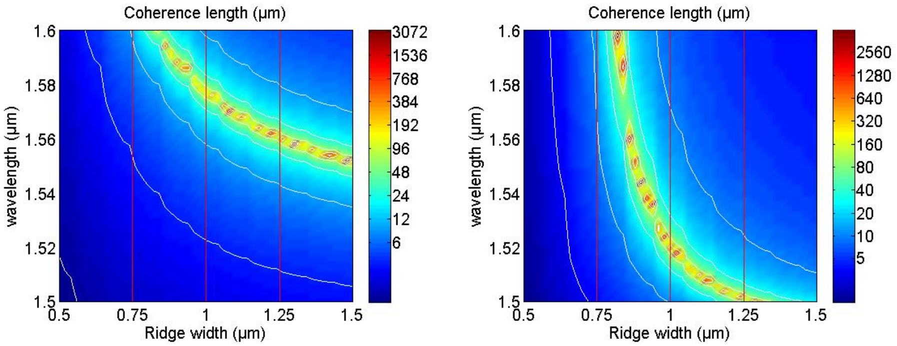

(a) **(b)**

Fig. 2. Coherence length versus λ_{FF} and w, for the suspended waveguide (a) and for the waveguide on an aluminium-oxide substrate (b).

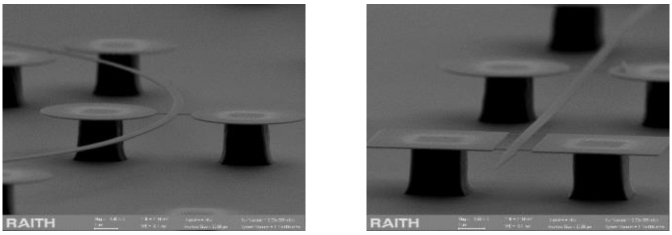

(a) **(b)**

Fig. 3. Scanning-electron-microscope pictures of a suspended waveguide: (a) bent geometry; (b) inverted taper for end-fire light coupling.

Ideal losses in snake waveguides are of two types: 1) radiation losses at the bent interface between the waveguide and the air; and 2) losses due to the non-ideal mode overlap at the waveguide sections where the sign of the snake curvature changes. Simulations performed with COMSOL on the suspended waveguides predict them to be smaller than 1dB/cm for w = 0.75 μm and R_c = 20 μm, as well as for w = 1 μm and R_c = 50 μm. In such waveguides, the calculated SHG conversion efficiencies are $\eta_{SHG} = 7\mathrm{x}10^3\ \mathrm{W}^{-1}\mathrm{cm}^{-2}$ and $\eta_{SHG} = 4.5\mathrm{x}10^3\ \mathrm{W}^{-1}\mathrm{cm}^{-2}$, respectively.

Although the overall losses also include scattering and residual absorption losses due to non-ideal fabrication and materials, their preliminary measurements show the good potential of high-index-contrast snake-shaped AlGaAs nanowires for three-wave mixing.

References:

[1] Y. Dumeige and P. Feron, “Whispering-gallery-mode analysis of phase-matched doubly resonant second-harmonic generation”, Phys. Rev. A 74, 063804 (2006).

[2] P. S. Kuo, J. Bravo-Abad, and G. S. Solomon, “Second-harmonic generation using $\bar{4}$-quasi-phasematching in a GaAs whispering-gallery-mode microcavity”, Nat. Commun. 5, 3109 (2014).

[3] S. Mariani, et al., “Second-harmonic generation in AlGaAs microdisks in the telecom range”, Optics Letters 39, 3062 (2014).

[4] R. T. Horn, and G. Weihs, “Directional Quasi-Phase Matching in Curved Waveguides”, arXiv: 1008.2190 (2010).